New Phytologist

Research

Stable carbon isotope labeling reveals different carry-over effects between functional types of tropical trees in an Ethiopian mountain forest

Julia Krepkowski[1], Aster Gebrekirstos[2], Olga Shibistova[3,4] and Achim Bräuning[1]

[1]Institute of Geography, University of Erlangen-Nuremberg, Kochstr 4/4, 91054, Erlangen, Germany; [2]World Agroforestry Centre, PO Box 30677, Nairobi, Kenya; [3]Institute of Soil Science, Leibniz University Hannover, Herrenhäuser Str 2, 30419, Hannover, Germany; [4]V.N.Sukachev Institute of Forest, Siberian Branch of the Russian Academy of Sciences, Akademgorodok, 660036, Krasnoyarsk, Russia

Author for correspondence:
Julia Krepkowski
Tel: +49 9131 8522638
Email: julia.krepkowski@geographie.uni-erlangen.de

Received: *21 January 2013*
Accepted: *1 March 2013*

New Phytologist (2013) **199:** 431–440
doi: 10.1111/nph.12266

Key words: carryover effect, dendrometer, Ethiopia, growth dynamics, stable carbon isotopes, tropical dendrochronology, wood anatomy.

Summary

- We present an intra-annual stable carbon isotope ($\delta^{13}C$) study based on a labeling experiment to illustrate differences in temporal patterns of recent carbon allocation to wood structures of two functional types of trees, *Podocarpus falcatus* (a late-successional evergreen conifer) and *Croton macrostachyus* (a deciduous broadleaved pioneer tree), in a tropical mountain forest in Ethiopia.
- Dendrometer data, wood anatomical thin sections, and intra-annual $\delta^{13}C$ analyses were applied.
- Isotope data revealed a clear annual growth pattern in both studied species. For *P. falcatus*, it was possible to synchronize annual $\delta^{13}C$ peaks, wood anatomical structures and monthly precipitation patterns. The labeling signature was evident for three consecutive years. For *C. macrostachyus*, isotope data illustrate a rapid decline of the labeling signal within half a year.
- Our $\delta^{13}C$ labeling study indicates a distinct difference in carryover effects between trees of different functional types. A proportion of the labeled $\delta^{13}C$ is stored in reserves of wood parenchyma for up to 3 yr in *P. falcatus*. By contrast, *C. macrostachyus* shows a high turnover of assimilates and a carbon carryover effect is only detectable in the subsequent year.

Introduction

Fractionations of stable carbon and oxygen isotopes ($\delta^{13}C$ and $\delta^{18}O$) in tree rings of many species in the temperate (Leavitt & Long, 1988; McCaroll & Loader, 2004; Etien *et al.*, 2008; Esper *et al.*, 2010; Kress *et al.*, 2010), boreal (Kagawa *et al.*, 2006a,b; Gagen *et al.*, 2007) and Mediterranean (Battipaglia *et al.*, 2010; De Micco *et al.*, 2012; Szymczak *et al.*, 2012) zones have been analyzed at inter- and intra-annual resolutions. Understanding of fixation, allocation and remobilization processes of $\delta^{13}C$ within an annual cycle and various plant compartments is a prerequisite for isotope dendroclimatology (Damesin & Lelarge, 2003; Helle & Schleser, 2004; Augusti *et al.*, 2006; Kagawa *et al.*, 2006a,b). Helle & Schleser (2004) illustrated a 'triphase seasonal $\delta^{13}C$ pattern in broad-leaf deciduous trees' with: $\delta^{13}C$ increase at the beginning of the vegetation period owing to a carryover effect of stored carbohydrates assimilated during the previous vegetation period; $\delta^{13}C$ decrease during the main vegetation period; and a slight increase of $\delta^{13}C$ at the very end of the vegetation period as a result of the changed carbohydrate metabolism of senescent leaves. Furthermore, Helle & Schleser (2004) assumed that the mid-section of the seasonal $\delta^{13}C$ variation is most affected by environmental factors and may be suitable for reconstruction of seasonal environmental changes. Kagawa *et al.* (2006a,b) investigated carbon translocation, storage, and remobilization in time and different plant compartments after $^{13}CO_2$ pulse labeling of *Larix gmelini* growing in the boreal zone. The results show that earlywood of tree rings contains photoassimilates from the previous summer and autumn as well as from the current season. Usually, only latewood represents the photoassimilates of the current summer and autumn, although a contribution of stored material cannot be totally excluded. Hence, 'carbon storage is a key mechanism behind autocorrelation in (isotope) dendroclimatology' (Kagawa *et al.*, 2006b). However, these results were obtained from tree saplings and the authors stress the necessity of carrying out respective experiments on adult trees, which might differ in their behavior (Kagawa *et al.*, 2006b). As evident from a recent review article on pulse-labeling studies (Epron *et al.*, 2012), comparable studies for tropical regions have not been assessed.

A number of studies have already successfully applied stable isotope approaches in tropical regions, most of them working on an annual resolution (Verheyden *et al.*, 2004; Robertson *et al.*, 2006; Gebrekirstos *et al.*, 2009; Brienen *et al.*, 2010; Fichtler *et al.*, 2010; Wils *et al.*, 2010; Gebrekirstos *et al.*, 2011a, 2012;

Williams *et al.*, 2011). For instance, a significant negative correlation between annual precipitation and $\delta^{13}C$ time series of tree rings was found for several broadleaved tree species in various tropical climates (Fichtler *et al.*, 2010). Gebrekirstos *et al.* (2011b, 2012) found significant negative correlations of annual $\delta^{13}C$ and $\delta^{18}O$ variations in West African Sahel woodland species with precipitation amount, humidity, drought (Palmer drought severity index, PDSI), and positive correlations with temperature. Despite those encouraging correlations with climate parameters, physiologically based understanding of $\delta^{13}C$ variations in different tree species and functional types is still incomplete.

Stable isotopes have also been used to prove the annual nature of tree rings, to verify visually indistinct growth ring boundaries, and to delineate annual growth layers when visible tree rings are not present in tropical wood (Evans & Schrag, 2004; Poussart & Schrag, 2005; Anchukaitis *et al.*, 2008; Roden, 2008; Pons & Helle, 2011). Anatomically indistinct rings of two tree species growing in the tropical rainforest of central Guyana were identified as annual by Pons & Helle (2011). They used minima of intra-annual $\delta^{18}O$ and $\delta^{13}C$ variations as primary and secondary indicators of annual growth boundaries, verified by simultaneously measured diameter increment rates of the same trees. However, retrospective stable isotope analyses lack a precise time control when the respective part of the xylem was formed. High-resolution electronic dendrometers are a tool to register the dynamics of stem diameter incremental growth with great precision (Volland-Voigt *et al.*, 2011; Krepkowski *et al.*, 2011), thus providing a time control for the wood formed at a certain distance from the initial starting point of the measurements. Nevertheless, stem diameter increment alone cannot unambiguously be considered as an indicator of cambial growth (Krepkowski *et al.*, 2011, 2012). Positive radial change may result from stem swelling as a result of water uptake and saturation of wood tissues after dry periods; cambial activity with formation of new cells; or enlargement of juvenile cells before lignification (Deslauriers *et al.*, 2009; Krepkowski *et al.*, 2011). Hence, wood anatomical indications of cell formation have to be included for determination of periods of active cambium.

Here, we study differences in carbon carryover effects between different tree functional types linked with dendrometer measurements and wood anatomy to expand our understanding of tropical dendrochronology. To this end, we studied two native tree species with contrasting physiological traits in a tropical mountain forest in Ethiopia. *Podocarpus falcatus* is a late-successional evergreen conifer, while *Croton macrostachyus* is an early-successional deciduous tree, but seedlings and saplings of both species compete on the same sites after forest disturbance (Tesfaye *et al.*, 2010). In contrast to *P. falcatus*, *C. macrostachyus* shows a shorter life span, higher rates of photosynthesis and transpiration, a higher metabolic activity, and a higher transfer rate of phloem sugars to arbuscular mycorrhiza fungi in the soil (Seyoum *et al.*, 2012; Shibistova *et al.*, 2012). We hypothesize that in the case of the early-successional deciduous tree, the allocation of recently assimilated carbon from the tree canopy to wood will be faster than in the late-successional gymnosperm, and that as a result of the more conservative life strategy, the carryover effect will be more pronounced in the gymnosperm tree. In addition, we propose that intra-annual ^{13}C allocation patterns are related to wood anatomical structures that might indicate annual growth boundaries.

The specific objectives of the study were to analyze the intra-annual patterns of recent ^{13}C allocation in wood of tropical trees belonging to different functional types in order to detect differences in carbon carryover effects; to study differences in cambial dynamics and wood formation of the two studied tree species; and to investigate the relationships among intra-annual $\delta^{13}C$ variations, wood anatomical structures and moisture availability.

Materials and Methods

Study area

The study site is located in the Munessa-Shashamene Forest, a tropical mountain forest located 240 km south of Addis Ababa at the eastern escarpment of the Main Ethiopian Rift Valley (7°26′ N 38°53′E). The vegetation of the remnant natural forest is dominated mainly by the canopy species *Croton macrostachyus* Hochst. ex Del (143 trees ha^{-1}) and *Podocarpus falcatus* (73 trees ha^{-1}), but with the presence of other indigenous tree species (*Celtis africana* Burm.f., *Syzygium guineense* (Willd.) DC., and *Prunus africana* (Hook.f.) Kalkman (Tesfaye *et al.*, 2010)).

The climate is subhumid with mean annual temperatures of 14.9°C (minimum 14.3°C, maximum 15.4°C) and the annual rainfall averages 1225 mm with a standard deviation of 217 mm. The precipitation distribution is characterized by a bimodal rainfall pattern (Fritzsche *et al.*, 2006; Freier *et al.*, 2010), with alternate rainy and dry seasons: a long and intense rainy season from July to October followed by a long dry season from November to February and an unreliable short rainy season from March to June delimited by a short dry period in June (Krepkowski *et al.*, 2011). Recently, Strobl *et al.* (2011) reported that 'the gap between the small and the long rains [the short dry season] has disappeared and the climate in general has become more humid' during the last 9 yr.

Maximum air temperatures of 28.1°C occur at the end of the long dry season as a result of the rising position of the sun and low cloudiness accompanied by minimum air humidity. During the dry season, relative air humidity ranges between 45 and 75% and increases with the onset of the long rainy season to maximum values of 90%. The long-term climate data recorded *c.* 500 m from our study site indicated a high intra-annual precipitation variability with the occurrence of a distinct short dry season in April and May 2008 and 2009, as well as an indistinct long dry season in 2009–10 with many rain events during the period December 2009 to February 2010.

Soils in the area are derived from intermediate volcanic rocks that are present throughout the study area and are rich in clay and iron oxides. Plots under investigation are classified as Mollic Nitisol according to the World Reference Base of Soil Resources (FAO, ISRIC & ISSS, 1998).

Study species

Two indigenous tree species belonging to different functional types were selected for the study. The conifer *P. falcatus* (Podocarpaceae) can grow up to 40 m high and is characterized by a lobate stem form (Fig. 1a). *P. falcatus* is a shade-tolerant climax species constituting the dominant species in the upper story of the forest canopy (Tesfaye *et al.*, 2010). *P. falcatus* continuously produces new leaves in moist conditions, with a life span of an individual leaf exceeding 2 yr (Seyoum *et al.*, 2012).

By contrast, *C. macrostachyus* (Euphorbiaceae, Fig. 1d) is a shade-intolerant pioneer species growing in canopy gaps and occupying the middle and upper levels of the canopy (Tesfaye *et al.*, 2010; Shibistova *et al.*, 2012). Leaf fall of the deciduous *C. macrostachyus* begins at the end of the long dry season (January/February) and may extend until March/April, so that the leafless period lasts 3–4 months. Leaf flush occurs from March to June, followed by a vegetation period of 7 months (Tesfaye *et al.*, 2011; Seyoum *et al.*, 2012). Development of an individual *Croton* leaf requires up to 2 months, with a mean life span of only 3 months (Seyoum *et al.*, 2012).

Fig. 1(b, c) illustrates the wood anatomical structures of *P. falcatus* and *C. macrostachyus*, following the terminology of Schweingruber *et al.* (2006). The conifer tree (Fig. 1b) shows distinct ring boundaries in the form of rather narrow bands of radially flattened tracheids with slightly thickened cell walls in the latewood. Additionally, intra-annual density fluctuations (IADFs) are found, but the occurrence of these false rings is irregular and varies among years as well as among tree individuals (Krepkowski *et al.*, 2011). The cross-section of *C. macrostachyus* reveals wood structures typical for hardwoods with small and thick-walled fibers, a diffuse ring-porous structure with large vessels and wood rays one or two cell rows wide. Growth ring boundaries are marked by slightly thickened cells (Fig. 1c), but they are hard to identify. Occasionally, macroscopically visible tangential parenchyma bands occur and provide additional markers for growth ring boundaries.

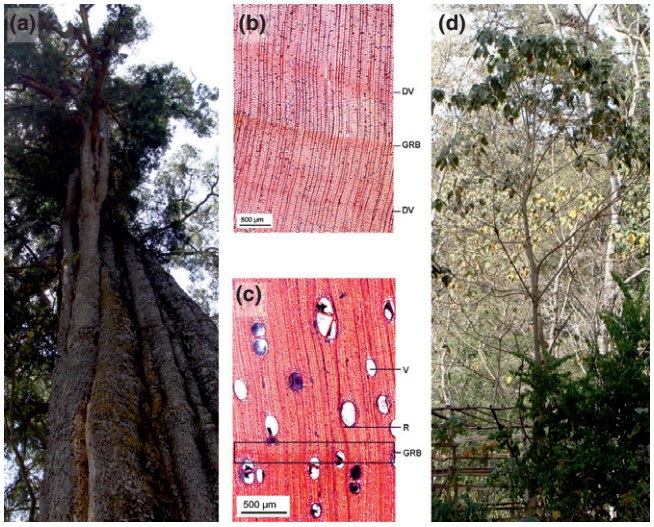

Fig. 1 (a) Photograph of an adult *Podocarpus falcatus* with a lobate stem. (b) Wood anatomical structure of *P. falcatus*. The tentative growth ring boundaries (GRB) and intra-annual density fluctuations (IADF) are formed by radially flattened and slightly thick-walled tracheids (Krepkowski *et al.*, 2011, see also Fig. 3). (c) Wood anatomical structure of *Croton macrostachyus* with vessels (V), rays (R) and hardly distinguishable GRB marked by slightly thickened cells. (d) Photograph of a middle-aged *C. macrostachyus*. [Correction added after online publication 16 April 2013: photograph (b) was replaced showing that the GRB and IADF are formed from tracheids.]

Dendrometer measurements and wood anatomy

Electronic point dendrometers (Ecomatik, Germany) were installed in March and September 2008 at 1–1.5 m height on the stems of various-sized *P. falcatus* and *C. macrostachyus* (six per species). Before fixation of the dendrometers, the outer parts of the trees' bark were removed to avoid the influence of swelling or shrinking of bark material on the dendrometer curves. Radial stem diameter variations were registered automatically in 30 min intervals. Diurnal stem diameter changes result mainly from changes of the tree's water status. Furthermore, long-term growth trends are recorded that help in determining periods of cambial activity and wood formation (Biondi *et al.*, 2005; Bräuning *et al.*, 2008, 2009; Volland-Voigt *et al.*, 2011; Krepkowski *et al.*, 2011, 2012). In addition, from 2008, wood microcores were collected at intervals of 3–6 wk with a trephor microcorer (Costruzioni Meccaniche Carabin C., Belluno, Italy) to study cambial activity in more detail (Rossi *et al.*, 2006). All microcores were stored in a solution of 50% ethanol in the field. In the laboratory, they were embedded in paraffin by means of dehydration (a mixture of ethanol and D-limonene) and successive infiltration of melted paraffin (Rossi *et al.*, 2006). Thereafter, sections of thickness 10–30 µm were cut with a rotation microtome (Leica, Wetzlar, Germany), cleaned of the remaining paraffin and finally stained with solutions of astra blue and safranin red to distinguish living and nonlignified cells (in blue) from lignified structures (in red). Finally, the dried thin sections were photographed with a Leica microscope system at fourfold magnification and the pictures were edited using Adobe Photoshop software.

Pulse labeling

Short-term $^{13}CO_2$ pulse labeling of the two target trees was carried out on two cloudless days (12 and 14 November 2008) at the start of the main rainy season. For the experiment, *c.* 6-m-high rectangular frames made of eucalyptus poles were constructed around the individual *P. falcatus* and *C. macrostachyus* trees, covering a surface of 12.7 and 16.7 m^2 for the former and latter, respectively. Shortly before the labeling event, a plastic glasshouse cover (120 µm, 88% light transmission in photosynthetically active radiation (PAR); UVA Clear, Ginegar Plastics Products Ltd, Kibbutz Ginegar, Israel) was pulled over the frame and tightly sealed within 30 min. To prevent transport of $^{13}CO_2$ from the chamber space into soil pores, the chamber was also sealed with the plastic film from the bottom side at 1.60 m distance from the forest floor. Corresponding chamber volumes were 58.4 m^3 for *C. macrostachyus* and 71.1 m^3 for *P. falcatus*. During the experiment, five electric fans (12 V,

0.21 A) circulated the air in the chambers and CO_2 concentration, air temperature, and relative humidity were monitored continuously using a LI-8100 infrared gas analyzer (Li-Cor Inc., Lincoln, NE, USA). Fifteen minutes after the chambers were sealed, and the decline of the CO_2 concentration inside the chambers clarified carbon dioxide uptake, ^{13}C-labeled CO_2 was generated by injecting diluted sulfuric acid into a flask containing isotopically enriched $Na_2{}^{13}CO_3$ solution (99 atom% ^{13}C), and 12.5 mM of $^{13}CO_2$ per 1 m^3 was added to each chamber (0.73 mol $^{13}CO_2$ for *C. macrostachyus* and 0.89 mol to *P. falcatus*) The labeling duration was 85 and 105 min for *C. macrostachyus* and *P. falcatus*, respectively, depending on the rate of the $^{12/13}CO_2$ concentration decrease within the chamber, to prevent an unnoticed loss of the tracer by respiration.

Wood sample collection and isotopic measurements

Wood samples of the labeled trees and control trees of similar size were collected with an increment borer (0.5 cm diameter, Suunto, Vantaa, Finland) in March 2011 (*P. falcatus* control was sampled in March 2009). After drying, sanding and polishing, the cores were photographed with a Leica stereoscope and camera system. Increment cores were cut with a modified rotation microtome (Leica) in thin sections of 30–40 µm thickness. Each section was collected separately in Eppendorf tubes and they were numbered consecutively. Every third thin section was packed in tin capsules and the $\delta^{13}C$ of whole wood was analyzed with a mass spectrometer (Delta V Advantage, Thermo Electron, Bremen, Germany). For high-resolution $\delta^{13}C$ analyses we used whole wood instead of α-cellulose, because, during the α-cellulose extraction process, *c.* 60–70% (Loader *et al.*, 1997) of the sample mass is lost, leading to insufficient amounts of remaining cellulose for mass spectrometry (Kagawa *et al.*, 2006a,b; Pons & Helle, 2011). Numerous studies (Barbour *et al.*, 2001; McCarroll & Loader, 2004; Helle & Schleser, 2004; English *et al.*, 2011; Pons & Helle, 2011 and references therein) have used whole wood and have revealed a constant offset of $\delta^{13}C$ of whole wood and cellulose for conifer wood of *c.* 1‰ (Warren *et al.*, 2001; Pons & Helle, 2011), so that no bias in the measured isotope variations was expected, as the labeling effect that leads to isotope signals *c.* 30–140 ‰ above the normal fractionation signal by far exceeds the naturally occurring variability of carbon isotopes in wood. Isotope values were calibrated with a laboratory standard (Pepton II) and expressed in δ notation (‰), relative to the Vienna Pee Dee Belemnite (VPDB) standard.

Results

Dendrometer data and microcores

The dendrometer curves of the six sampled *P. falcatus* (Fig. 2) show corresponding responses of fast or slow increment and stem shrinkage during wet and dry periods, respectively. Stem diameter increment occurs during the short rainy season after the first rainfall events at the end of the dry period (e.g. March and April 2009). The main growing period occurs during the long rainy season beginning around June. Despite the lack of dendrometer data at the end of the long rainy season in 2008, we delimit the growing period to the beginning of the dry season in November, as stem diameters before and after the data gap show almost identical values. By contrast, the main long rainy season of 2009 lasted until the end of October, followed by an indistinct long dry season with unusual rain events in December, inducing ongoing increment until a dryer period in February 2010.

A series of continuously sampled microcores of 'Podo A01' are shown in Fig. 3. All samples show growth ring boundaries formed during the long dry season of the years 2006, 2007 and 2008. The distinctness and width of the tree rings vary between the samples in the tangential direction as a result of lobate growth. The microcores illustrate periods of cambial activity in more detail. For example, in March 2009 the thin section depicts freshly formed cells, indicating an active cambium during the short rainy season (precipitation data are shown in Fig. 2). Hence, an IADF is visible in the following samples (IADF, 2009) caused by dormancy of the cambium during the short dry season in April and May 2009. Following the onset of the long rainy season in June 2009, the thin sections from June and September show bands of bluish-colored freshly formed unlignified cells. After a period of lower cambial activity or beginning dormancy in October 2009, the thin section from December 2009 again indicates an active cambium inducing a missing growth ring boundary in this year. Cambial activity

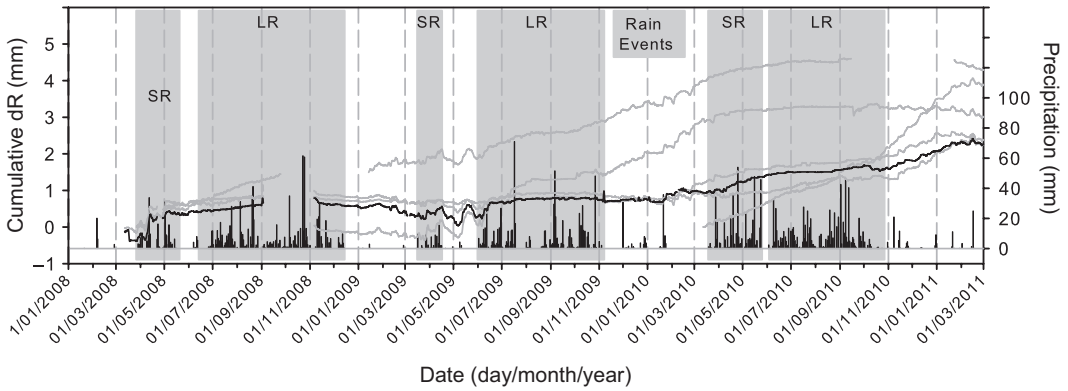

Fig. 2 Cumulative daily radial diameter change (d*R*) of six *Podocarpus falcatus* from March 2008 to March 2011. 'Podo A01' is shown by a continuous line and 'Podo A02, A03, A04, E04, E05' by dashed lines. Duration of the short (SR) and long (LR) rainy seasons and further rain events are colored in gray. All sampled individuals react synchronously to wet and dry periods with stem increment and shrinkage, respectively.

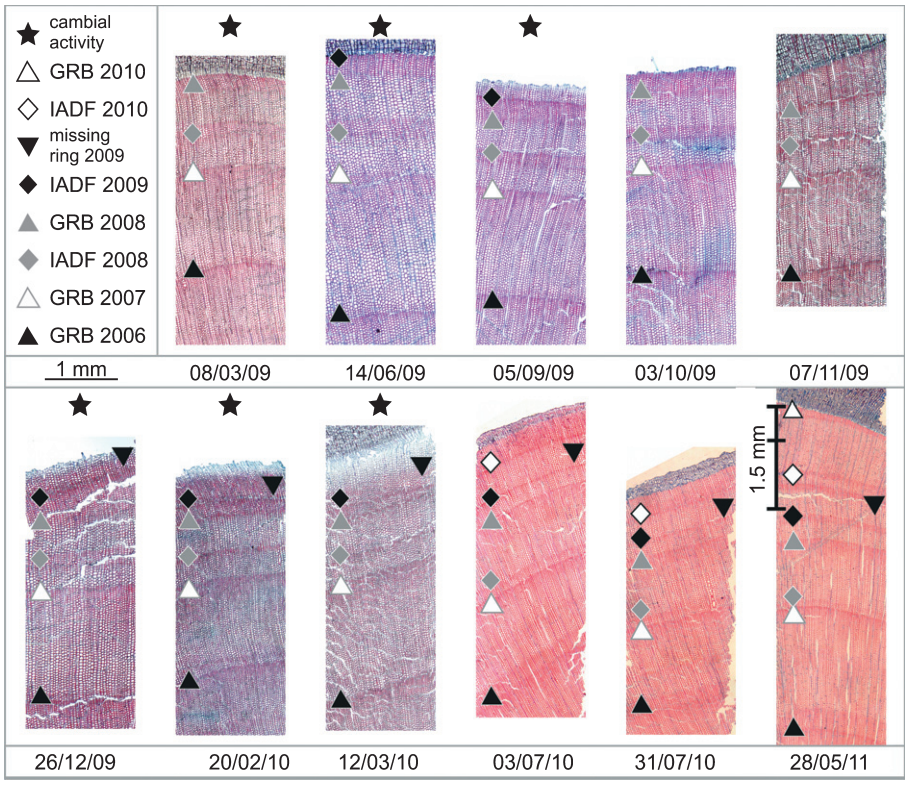

Fig. 3 Thin sections of *Podocarpus falcatus* 'Podo A01' collected at different dates for analyzing cambial activity. The symbols mark growth ring boundaries (GRBs) and intra-annual density fluctuations (IADFs) of different years: black, white and gray triangles highlight GRBs of 2006, 2007 and 2009, respectively; gray, black and white diamonds highlight IADFs of 2008, 2009 and 2010, respectively. Samples of March, June, September, and December 2009, and February and March 2010 show bluish-stained parts of juvenile cells illustrating cambial activity (black star). The missing ring boundary of the more humid long dry season 2009–10 is depicted by a black triangle. The number of earlywood cell rows between the thickened latewood cells (GRB or IADF) varies between samples as a result from the irregular and lobate stem growth of *P. falcatus* (e.g. number of cell rows between GRB 2006 and 2007 in samples of February and March 2010). The scale in the thin section from May 2011 illustrates a total increment of 1.5 mm in 2 yr.

continued until a drier period in June 2010 and a new IADF is visible in the samples of July 2010 and May 2011.

The dendrometer data of the six sampled *C. macrostachyus* (Fig. 4) indicate that all trees react synchronously to the local rainfall pattern. After a stem diameter minimum during the short dry season April–May 2009, increment started after complete refoliation and continued until November 2009. Owing to the ample rain events during the long dry season 2009–10, leaf flush of *C. macrostachyus* occurred earlier in 2010 and stem diameter increment had already started in the middle of March 2010.

Owing to the wood anatomy of *C. macrostachyus*, growth ring boundaries are hard to identify. Therefore, only similar wood structures of slightly thickened cells are marked in Fig. 5. The thin sections of May, June, and September 2009 indicate cambial activity by rows of new cells in blue. Corresponding to the dendrometer data and an earlier leaf flush in 2010, freshly formed cell rows are already visible in April 2010.

Intra-annual variations of tree-ring $\delta^{13}C$

High-resolution intra-annual $\delta^{13}C$ analyses are illustrated in Table 1 and Figs 6 and 7. Before the labeling experiment, both *P. falcatus* trees showed similar average $\delta^{13}C$ values and intra-annual ranges (unlabeled tree, $-24.96 \pm 0.99‰$, range -26.80 to $-22.97‰$; labeled tree, $-25.13 \pm 0.83‰$, range -27.06 to $-22.90‰$; $P = 0.15$, not significant). An individual range in $\delta^{13}C$ of 1–3‰ was also found in other species (Saurer *et al.*, 1997; Gebrekirstos *et al.*, 2009; Esper *et al.*, 2010) and is influenced by site conditions (microclimate) and possibly tree age. After labeling, $\delta^{13}C$ reaches extremely high positive values of up to 122.23‰ and stable isotope ratios in wood remain at elevated values for the following three annual cycles (Fig. 6). In labeled and control trees, peaks of $\delta^{13}C$ can be aligned to distinct wood anatomical structures of tracheids with thickened cell walls. In Fig. 6, precipitation data of September 2008 to November 2009 were aligned to the isotope data of the labeled *P. falcatus*. The $\delta^{13}C$ peak around the growth ring boundary of 2008 coincides with minimum precipitation during the long dry season 2008–09. Moreover, the dry conditions in May 2009 (short dry season 2009) induced a second peak of $\delta^{13}C$ in the annual cycle. On the other hand, $\delta^{13}C$ values decrease towards an annual minimum during the long rainy season (July–October 2009).

The $\delta^{13}C$ values of both *C. macrostachyus* samples show high intra-annual variations with a distinct peak and an annual amplitude of *c.* 2.5‰. The mean annual $\delta^{13}C$ values of control and labeled *C. macrostachyus* before the labeling experiment were $-28.26 \pm 0.55‰$ and $-26.65 \pm 0.56‰$, respectively. Values of the unlabeled tree were higher, but show similar cyclic fluctuations as the labeled tree. After the labeling experiment, $\delta^{13}C$ increased up to $-1.51‰$ and the labeling signature decayed during the following year (Fig. 7). No anatomical wood structures can be visually matched with the $\delta^{13}C$ cycle. Precipitation data could not be reliably aligned to the $\delta^{13}C$ data.

Discussion

Cambial dynamics of different functional tree types

The wood anatomical thin sections demonstrate that *P. falcatus* can have repeated phases of cambial activity of different length

New Phytologist

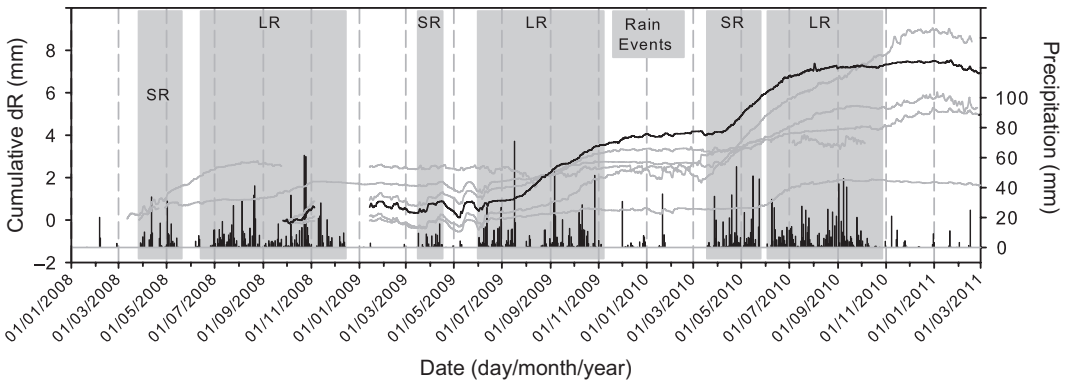

Fig. 4 Cumulative daily radial diameter change (d*R*) of six *Croton macrostachyus* from March or September 2008 to March 2011. 'Croton G02' is shown by a continuous line and 'Croton, G01, G03, G04, C02, D03' by dashed lines. Duration of the short (SR) and long (LR) rainy seasons and further rain events are colored gray. All sampled individuals react synchronously to wet and dry periods with stem increment and shrinkage, respectively.

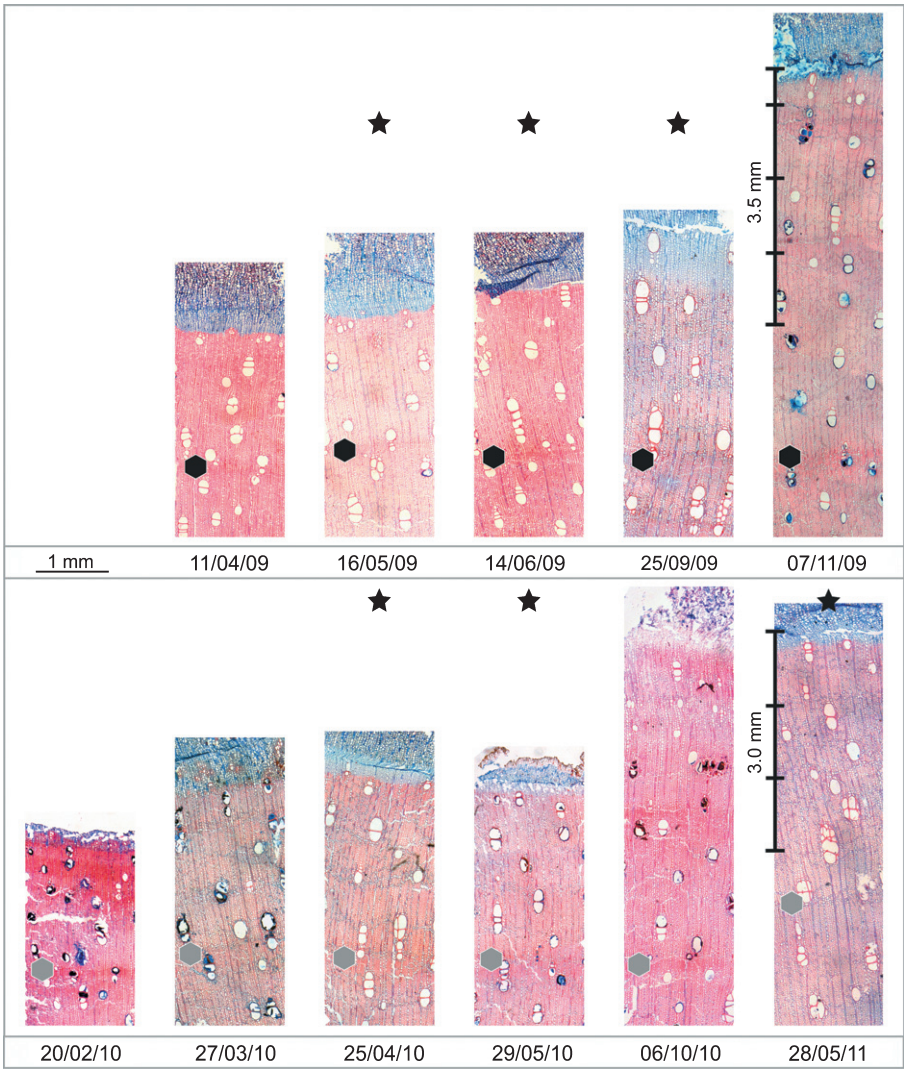

Fig. 5 Thin sections of *Croton macrostachyus* 'Croton G02' extracted at different dates for analyzing cambial activity. The symbols (black and gray hexagons) mark identical wood structures of assumed identical age in different samples. Samples from May, June, and September 2009, April and May 2010 and May 2011 show bluish-stained juvenile cells, illustrating cambial activity (black stars). Ring boundaries could not be determined. Scales in thin sections from November 2009 and May 2011 document annual increments of 3.5 and 3 mm, respectively.

within 1 yr. Cambium was active during the short rainy season (March 2009 and 2010), the long rainy season (June 2009 and September 2009), and occasionally even during the long dry season if there was sufficient rainfall (December 2009 and February 2010). On the other hand, phases of cambial dormancy are also implicated and result in distinct growth ring boundaries, but also in indistinct and multiple intra-annual density fluctuations (Krepkowski *et al.*, 2012). By contrast, the broadleaved evergreen

Table 1 Whole wood $\delta^{13}C$ mean with standard deviation (SD), and maximum and minimum values of increment cores

	$\delta^{13}C$ (‰, VPDB)		
	Mean with SD	Maximum	Minimum
Podocarpus falcatus control	−24.96 ± 0.99	−22.97	−26.80
P. falcatus labeled			
Before labeling	−25.13 ± 0.83	−22.90	−27.06
After labeling	−8.75 ± 33.72	122.23	−26.64
Croton macrostachyus control	−28.26 ± 0.55	−26.87	−29.37
C. macrostachyus labeled			
Before labeling	−26.65 ± 0.56	−25.58	−28.05
After labeling	−23.86 ± 7.29	−1.51	−27.85

VPDB, Vienna Pee Dee Belemnite.

P. africana forms one growth ring boundary yr^{-1} (Krepkowski *et al.*, 2011), indicating differences in cambial phenology between evergreen tree species.

In agreement with the leaf phenological studies of Tesfaye *et al.* (2010) and Seyoum *et al.* (2012), cambial activity in the broadleaved deciduous *C. macrostachyus* normally begins with the onset of the long rainy season around June (e.g. 2009). Generally, stem diameter increment before this date is the result of water re-saturation of wood tissues, except under humid conditions during the long dry season (e.g. in 2009–10), inducing an earlier leaf exchange and start of the growing season. Cambial dormancy and growth ring boundary formation at the end of the long rainy season are similar to the co-occurring deciduous *C. africana* (Krepkowski *et al.*, 2011), but the growth boundary is more distinct in *C. africana*. It is worth noting that a detailed review of tree ring studies in the lowlands and highlands of Ethiopia (Wils *et al.*, 2011) highlighted the complexity of ring formation and identified four major types of growth ring expression: anatomically not distinct rings, multiple rings yr^{-1}, annual rings and multiple missing rings associated with the local precipitation regime (unimodal to multimodal) and species sensitivity to water availability.

Linking intra-annual stable isotope variation, wood anatomy and climate

Because of the wood anatomy of *P. falcatus*, with the formation of false rings, and *C. macrostachyus*, showing indistinct growth boundaries, the establishment of cross-dated ring-width chronologies from synchronized growth curves has not yet been successful. Our study of $\delta^{13}C$ in whole wood indicates an annual pattern with a distinct peak of $\delta^{13}C$ for both species and sampled individuals (labeled and control; Figs 6 and 7). Maxima of $\delta^{13}C$ in *P. falcatus* can be visually correlated to latewood cells with higher cell wall thickness or to growth ring boundaries, and thus can be helpful for further dendrochronological studies. The annual peak of $\delta^{13}C$ coincides with the beginning of the long dry season and thus with environmental conditions characterized by low relative humidity, high vapor pressure deficit or low soil

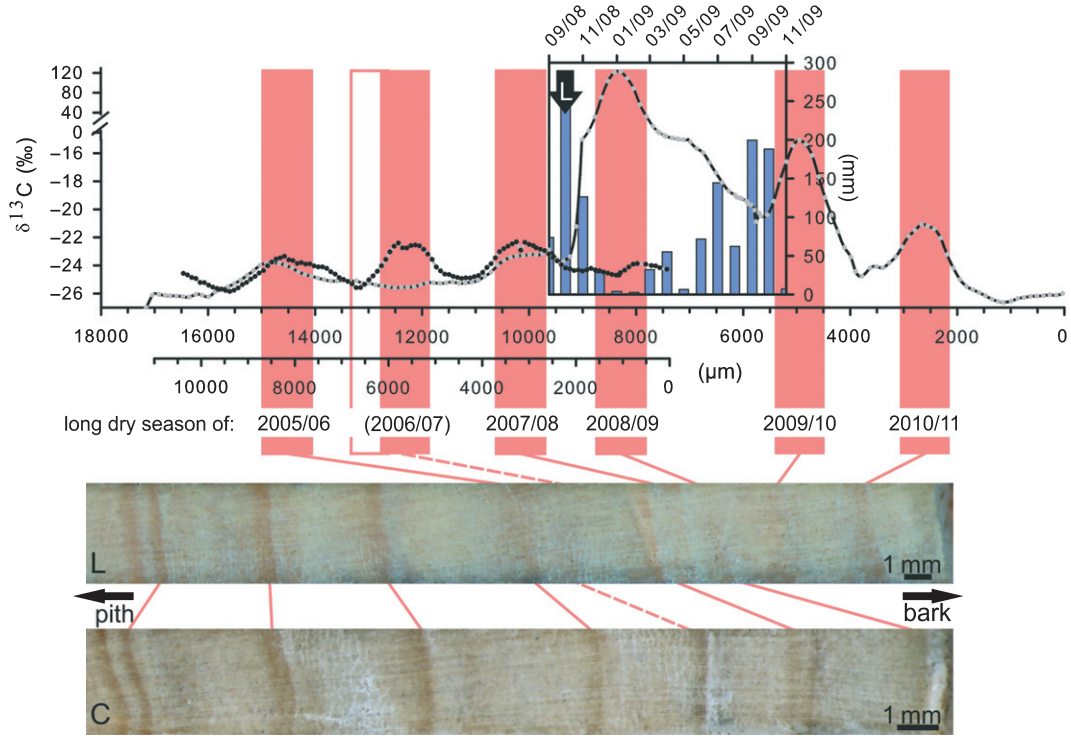

Fig. 6 Whole wood $\delta^{13}C$ of labeled (black line with gray dots) and control (gray line with black dots) *Podocarpus falcatus* with precipitation data from September 2008 to November 2009 aligned to the isotope data of the labeled *P. falcatus*. Black arrow points to the date of the labeling experiment. Red bars indicate peak $\delta^{13}C$ values controlled by the long dry season and are correlated to corresponding wood structures in labeled (L, extracted on 29 March 2011) and control (C, extracted on 14 March 2009) *P. falcatus*.

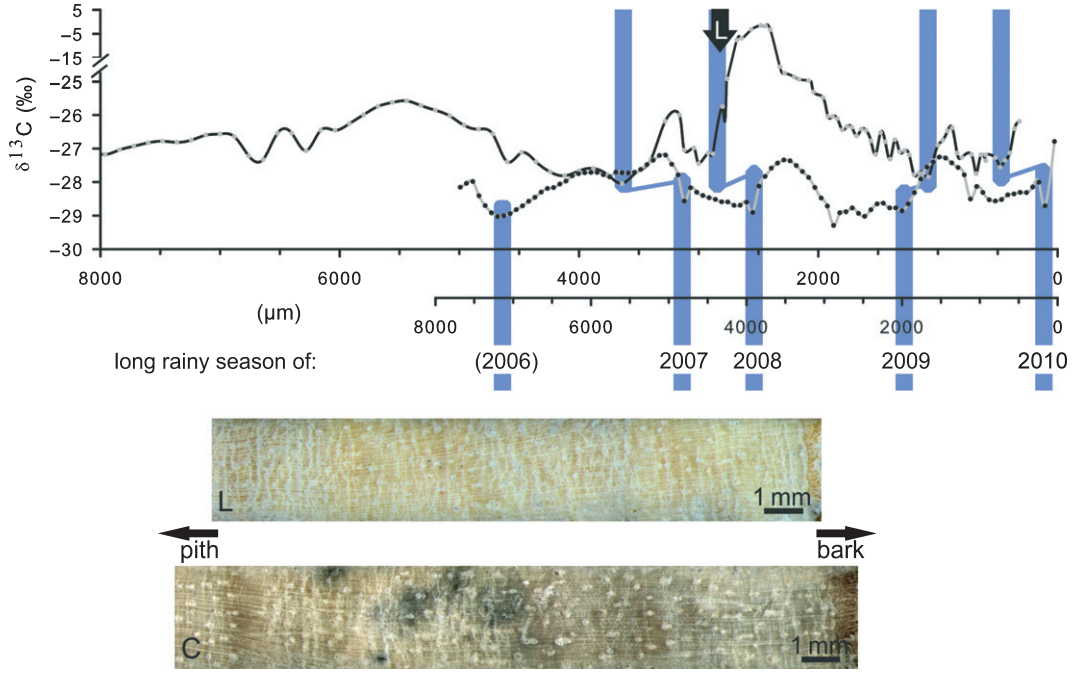

Fig. 7 Whole wood $\delta^{13}C$ of labeled (black line with gray dots) and control (gray line with black dots) *Croton macrostachyus*. The black arrow highlights the date of the labeling experiment. Blue bars indicate annual minimum $\delta^{13}C$ values controlled by the long rainy season. Labeled (L) and control (C) increment cores of *C. macrostachyus* were extracted on 29 March 2011 and 7 March 2011, respectively.

moisture. In 2009, a second, smaller $\delta^{13}C$ peak occurred in the labeled *P. falcatus*, which corresponds to the occurrence of a short dry season. Thus, primary and secondary maxima of $\delta^{13}C$ reflect the tree's reaction to dry climate conditions by stomatal closure and decreased discrimination against ^{13}C during photosynthesis. Although our sample size is not sufficient for statistical analysis, the visual correspondence between isotope variations and climate data in Fig. 6 encourages further dendroecological isotope studies, potentially verifying the negative correlation between moisture and $\delta^{13}C$ discrimination.

In contrast to the conifer species, $\delta^{13}C$ peaks of *C. macrostachyus* occur in the earlywood. This probably corresponds to the beginning of the growing season, as initial earlywood formation in broadleaved species is often accompanied by the mobilization of stored carbohydrates with a subsequent rise of $\delta^{13}C$ (Hill *et al.*, 1995; Barbour *et al.*, 2002; Fichtler *et al.*, 2010). After refoliation and the beginning of the growing season around June 2009, the downward trend of $\delta^{13}C$ (Fig. 7) is more or less synchronous to increasing precipitation during the long rainy season from June to November 2009 (Fig. 7). Hence, this period of the annual $\delta^{13}C$ cycle may correspond to the 'midsection of the seasonal $\delta^{13}C$ variation' *sensu* Helle & Schleser (2004). Owing to the indistinct formation of annual rings in the cores of *C. macrostachyus*, it was not possible to assign intra-annual stable isotope variations to distinct wood anatomical structures.

The cyclic intra-annual $\delta^{13}C$ variations in the wood of *P. falcatus* may be used to identify annual growth ring boundaries. As has also been shown by Poussart & Schrag (2005) for other *Podocarpus* species from Thailand, intra-annual variations of $\delta^{13}C$ can also help to distinguish tree-ring boundaries. By contrast, $\delta^{13}C$ variations in the wood of *C. macrostachyus* did not allow a clear delimitation of growth rings, as was reported for other tropical broadleaved species by Pons & Helle (2011). In such cases, intra-annual $\delta^{18}O$ variations may be used as additional evidence for the detection of annual growth layers (Evans & Schrag, 2004; Anchukaitis *et al.*, 2008; Pons & Helle, 2011).

Carbon carry-over effects in different tree functional types

Both study species show a distinct reaction in the $^{13}CO_2$-labeling experiment. Despite the comparable amount of ^{13}C assimilated by *C. macrostachyus* and *P. falcatus* foliage during the labeling experiment (5.9 ± 0.3 and 6.9 ± 1.3 g, respectively; Shibistova *et al.*, 2012), the proportion and temporal pattern of the tracer allocation to the wood tissues and carbohydrates in the phloem sap differed between the tree species. Phloem sap velocity was *c.* four times higher for *C. macrostachyus.* We found a rapid increase of $\delta^{13}C$ in *P. falcatus*, with a maximum of 122‰ in thickened latewood cells of 2008, indicating a formation of latewood mainly from photoassimilates of the current growing season. Furthermore, earlywood and latewood of the two consecutive growing seasons show increased $\delta^{13}C$ values, but with a gradual decline towards the natural value of *c.* −25‰ in spring 2011. The estimated life span of *P. falcatus* needles is up to 3 yr (Seyoum *et al.*, 2012), which coincides with the decay of the labeling signal in the wood. On the other hand, Shibistova *et al.* (2012) found that the $\delta^{13}C$ signal in labeled *P. falcatus* needles depleted and reached the value of the leaves of reference trees after 1 yr, whereas photosynthesis products (D-1-*O*-methyl-*muco*-inositol; OMMI) in phloem sap still showed isotopic enrichment of 2–10‰ after 1 yr. Hence, we assume that

P. falcatus makes use of storage carbohydrates remobilized from reserves in the wood parenchyma to form new xylem cells.

Remobilization of ^{13}C-enriched starch at the beginning of the growing period has been demonstrated for tropical tree species (Fichtler *et al.*, 2010; Pons & Helle, 2011) as well as for species of the temperate and boreal climate zones (Helle & Schleser, 2004; Kagawa *et al.*, 2006a,b; Gessler *et al.*, 2009). Comparably, while carryover effects for the pioneer *C. macrostachyus* are similar to deciduous trees in temperate climate zones (Helle & Schleser, 2004), they extend over more than one vegetation period in the late-successional conifer *P. falcatus*, similar to evergreen trees in the boreal zone (Kagawa *et al.*, 2006a,b). As the secondary metabolite OMMI, which is ubiquitous in gymnosperms, behaves more conservatively than the sucrose presented in angiosperm phloem sap (Shibistova *et al.*, 2012), the observed differences in carryover effects might also partly reflect general evolutionary traits. The extended carryover effect in evergreen species might also influence the climatic signal strength contained in δ^{13}C series. In eastern and western Africa, Gebrekirstos *et al.* (2009, 2012) found stronger climatic signals in deciduous species compared with co-occurring evergreen species.

Conclusions

We investigated a dominant late-successional evergreen conifer tree species and an early-successional deciduous broadleaved pioneer species in a tropical mountain forest in southern Ethiopia. Our study demonstrated that the functional types of tropical trees differ in their cambial phenology and use of stored carbohydrates for cell formation. The evergreen conifer is able to initiate wood formation at any time of the year when moisture conditions are sufficient, whereas cambial activity of the deciduous broadleaved species is restricted to the foliated period during the long rainy season.

Epron *et al.* (2012) reviewed 47 pulse-labeling studies mainly on beech and pine from temperate and boreal trees and concluded that the rate of transfer differs between broadleaved and coniferous species and generally decreases as temperature and soil water content decrease. Similarly, our δ^{13}C labeling study, the first of its kind in a tropical ecosystem, suggests distinct differences in carryover effects in tropical tree functional types. Whole wood δ^{13}C of *C. macrostachyus* shows a fast depletion of the isotope tracer within 1 yr. By contrast, the isotope signal can be detected over three vegetation periods in *P. falcatus*. This underlines the fact that a deeper knowledge of carbon storage strategies and ecophysiological processes is important to expand our understanding of tropical dendroclimatology. This difference in carbon allocation between early-successional deciduous pioneer species and late-successional conifers also has implications on plant–soil–atmosphere carbon balances of different forest successional stages, which have to be considered for carbon management of tropical forest landscapes. To gain a complete understanding of the different growth strategies and their ecological adaptations in the studied tropical mountain forest, the applied study approach should be extended to other tree functional types such as evergreen broadleaved trees.

Acknowledgements

We are indebted to the German Research Foundation for funding this project (BR 1895/15). We are grateful to the two anonymous reviewers for their constructive comments, which helped us to improve the quality of the paper.

References

Anchukaitis KJ, Evans MN, Wheelwright NT, Schrag DP. 2008. Stable isotope chronology and climate signal calibration in neotropical cloud forest trees. *Journal of Geophysical Research* **113**: G03030, doi:10.1029/2007JG000613.

Augusti A, Betson TR, Schleucher J. 2006. Hydrogen exchange during cellulose synthesis distinguishes climatic and biochemical isotope fractionations in tree rings. *New Phytologist* **172**: 490–499.

Barbour MM, Andrews TJ, Farquhar GD. 2001. Correlations between oxygen isotope ratios of wood constituents of *Quercus* and *Pinus* samples from around the world. *Australian Journal of Plant Physiology* **28**: 335–348.

Barbour MM, Walcroft AS, Farquhar GD. 2002. Seasonal variation in δ^{13}C and δ^{18}O of cellulose from growth rings of *Pinus radiata*. *Plant, Cell & Environment* **25**: 1483–1499.

Battipaglia G, De Micco V, Brand W, Linke P, Aronne G, Saurer M, Cherubini P. 2010. Variations of vessel diameter and ∂^{13}C in false rings of *Arbutus unedo* L. reflect different environmental conditions. *New Phytologist* **188**: 1099–1112.

Biondi F, Hartsough PC, Estrada IG. 2005. Daily weather and tree growth at the tropical treeline of North America. *Arctic, Antaractic and Alpine Research* **37**: 16–24.

Bräuning A, Homeier J, Cueva E, Beck E, Günter S. 2008. Growth dynamics of trees in tropical mountain ecosystems. *Ecological Studies* **198**: 291–302.

Bräuning A, Volland-Voigt F, Burchardt I, Ganzhi O, Nauss T, Peters T. 2009. Climatic control of radial growth of *Cedrela montana* in a humid mountain rainforest in southern Ecuador. *Erdkunde* **63**: 337–345.

Brienen RJW, Wanek W, Hietz P. 2010. Stable carbon isotopes in tree rings indicate improved water use efficiency and drought response of a tropical dry forest tree species. *Trees* **25**: 103–113.

Damesin C, Lelarge C. 2003. Carbon isotope composition of current-year shoots from *Fagus sylvatica* in relation to growth, respiration and use of reserves. *Plant, Cell & Environment* **26**: 207–219.

De Micco V, Battipaglia G, Brand W, Linke P, Saurer M, Aronne G, Cherubini P. 2012. Discrete versus continuous analysis of anatomical and ∂^{13}C variability in tree rings with intra-annual density fluctuations. *Trees* **26**: 513–524.

Deslauriers A, Giovannelli A, Rossi S, Castro G, Fragnelli G, Traversi L. 2009. Intra-annual cambial activity and carbon availability in stem of poplar. *Tree Physiology* **29**: 1223–1235.

English NB, McDowell NG, Allen CD, Mora C. 2011. The effects of α-cellulose extraction and blue-stain fungus on retrospective studies of carbon and oxygen isotope variation in live and dead trees. *Rapid Communications in Mass Spectrometry* **25**: 3083–3090.

Epron D, Bahn M, Derrien D, Lattanzi FA, Pumpanen J, Gessler A, Högberg P, Maillard P, Dannoura M, Gérant D, *et al.* 2012. Pulse-labelling trees to study carbon allocation dynamics: a review of methods, current knowledge and future prospects. *Tree Physiology* **32**: 776–798.

Esper J, Frank DC, Battipaglia G, Büntgen U, Holert C, Treydte K, Siegwolf R, Saurer M. 2010. Low-frequency noise in δ^{13}C and δ^{18}O tree ring data: a case study of *Pinus uncinata* in the Spanish Pyrenees. *Global Biogeochemical Cycles* **24**: GB4018.

Etien N, Daux V, Masson-Delmotte V, Stievenard M, Bernard V, Durost S, Guillemin MT, Mestre O, Pierre M. 2008. A bi-proxy reconstruction of Fontainebleau (France) growing season temperature from AD 1596 to 2000. *Climate Past* **4**: 91–106.

Evans MN, Schrag DP. 2004. A stable isotope-based approach to tropical dendroclimatology. *Geochimica et Cosmochimica Acta* **68**: 3295–3305.

FAO, ISRIC and ISSS. 1998. *World references base for soil resources*. Rome, Italy: Food and Agriculture Organization of the United Nations.

Fichtler E, Helle G, Worbes M. 2010. Stable-carbon isotope time series from tropical tree rings indicate a precipitation signal. *Tree-Ring Research* **66**: 35–49.

Freier KP, Glaser B, Zech W. 2010. Mathematical modelling of soil carbon turnover in natural *Podocarpus* forest and *Eucalyptus* plantation in Ethiopia using compound specific $\delta^{13}C$ analysis. *Global Change Biology* **16**: 1487–1502.

Fritzsche F, Asferachew A, Fetene M, Beck E, Weise S, Guggenberger G. 2006. Soil–plant hydrology of indigenous and exotic trees in an Ethiopian montane forest. *Tree Physiology* **26**: 309–320.

Gagen M, McCarroll D, Loader NJ, Robertson I, Jalkanen R, Anchukaitis KJ. 2007. Exorcising the "segment length curse": summer temperature reconstruction since AD 1640 using non-detrended stable carbon isotope ratios from pine trees in northern Finland. *Holocene* **17**: 435–446.

Gebrekirstos A, Bräuning A, Van Noordwijk M, Mitlöhner R. 2011b. Understanding past, present, and future climate changes from East to West Africa. *Agricultural Innovations for Sustainable Development* **3**: 77–86.

Gebrekirstos A, Mitlöhner R, van Noordwijk M, Bräuning A. 2012. Tracing responses to climate variability from stable isotopes in tree rings of *Anogeissus leiocarpus* and *Sclerocarya birrea* from the Sahel zone, Burkina Faso. *TRACE* **10**: 6–12.

Gebrekirstos A, Teketay D, Fetene M, Worbes M, Mitlöhner R. 2009. Stable carbon isotope ratios in tree rings of co-occurring species from semi arid tropics in Africa: patterns and climatic signals. *Global Planetary Change* **66**: 253–260.

Gebrekirstos A, van Noordwijk M, Neufeld H, Mitlöhner R. 2011a. Relationships of stable carbon isotopes, plant water potential and growth: an approach to assess water use efficiency and growth strategies of dry land agroforestry species. *Trees* **25**: 95–102.

Gessler A, Brandes E, Buchmann N, Helle G, Rennenberg H, Barnard RL. 2009. Tracing carbon and oxygen isotope signals from newly assimilated sugars in the leaves to the tree-ring archive. *Plant, Cell & Environment* **32**: 780–795.

Helle G, Schleser GH. 2004. Beyond CO_2-fixation by Rubisco – an interpretation of $^{13}C/^{12}C$ variations in tree rings from novel intra-seasonal studies on broad-leaf trees. *Plant, Cell & Environment* **27**: 367–380.

Hill SA, Waterhouse JS, Field EM, Switsur VR, Rees T. 1995. Rapid recycling of triose phosphates in oak stem tissue. *Plant, Cell & Environment* **18**: 931–936.

Kagawa A, Sugimoto A, Maximov TC. 2006a. $^{13}CO_2$ pulse-labelling of photoassimilates reveals carbon allocation within and between tree rings. *Plant, Cell & Environment* **29**: 1571–1584.

Kagawa A, Sugimoto A, Maximov TC. 2006b. Seasonal course of translocation, storage and remobilization of ^{13}C pulse-labeled photoassimilate in naturally growing *Larix gmelinii* saplings. *New Phytologist* **171**: 793–804.

Krepkowski J, Bräuning A, Gebrekirstos A. 2012. Growth dynamics and potential for crossdating and multi-century climate reconstruction of *Podocarpus falcatus* in Ethiopia. *Dendrochronologia* **30**: 257–265.

Krepkowski J, Bräuning A, Gebrekirstos A, Strobl S. 2011. Cambial growth dynamics and climatic control of different tree life forms in tropical mountain forest in Ethiopia. *Trees* **25**: 59–70.

Kress A, Saurer M, Siegwolf RTW, Frank DC, Esper J, Bugmann H. 2010. A 350-year drought reconstruction from Alpine tree-ring stable isotopes. *Global Biogeochemistry Cycles* **24**: GB2011, doi:10.1029/2009GB003613.

Leavitt SW, Long A. 1988. Stable carbon isotope chronologies from tree in the Southwestern United States. *Global Biogeochemistry Cycles* **2**: 189–198.

Loader NJ, Robertson I, Barker AC, Switsur VR, Waterhouse JS. 1997. An improved technique for the batch processing of small wholewood samples to α-cellulose. *Chemical Geology* **136**: 313–317.

McCarroll D, Loader NJ. 2004. Stable isotopes in tree rings. *Quaternary Science Reviews* **23**: 771–801.

Pons TL, Helle G. 2011. Identification of anatomically non-distinct annual rings in tropical trees using stable isotopes. *Trees* **25**: 83–93.

Poussart PF, Schrag DP. 2005. Seasonally resolved stable isotope chronologies from northern Thailand deciduous trees. *Earth and Planetary Science Letters* **235**: 752–765.

Robertson I, Loader NJ, Froyd CA, Zambatis N, Whyte I, Woodborne S. 2006. The potential of the baobab (*Adansonia digitata* L.) as a proxy climate archive. *Applied Geochemistry* **21**: 1674–1680.

Roden J. 2008. Cross-dating of tree ring $\delta^{18}O$ and $\delta^{13}C$ times series. *Chemical Geology* **252**: 72–79.

Rossi S, Anfodillo T, Menardi R. 2006. Trephor: a new tool for sampling microcores from tree stems. *IAWA Journal* **27**: 89–97.

Saurer M, Borella S, Schweingruber F, Siegwolf R. 1997. Stable carbon isotopes in tree rings of beech: climatic versus site-related influences. *Trees* **11**: 291–297.

Schweingruber FH, Börner A, Schulze ED. 2006. *Atlas of woody plant stems.* Berlin, Germany: Springer.

Seyoum Y, Fetene M, Strobl S, Beck E. 2012. Foliage dynamics, leaf traits, and growth of coexisting evergreen and deciduous trees in a tropical montane forest in Ethiopia. *Trees* **26**: 1495–1512.

Shibistova O, Yohannes Y, Boy J, Richter A, Wild B, Watzka M, Guggenberger G. 2012. Rate of belowground carbon allocation differs with successional habit of two afromontane trees. *PLoS ONE* **7**: e45540.

Strobl S, Fetene M, Beck EH. 2011. Analysis of the "shelter tree-effect" of natural and exotic forest canopies on the growth of young *Podocarpus falcatus* trees in southern Ethiopia. *Trees* **25**: 769–783.

Szymczak S, Joachimski MM, Bräuning A, Hetzer T, Kuhlemann J. 2012. Are pooled tree ring $\delta^{13}C$ and $\delta^{18}O$ series reliable climate archives? A case study of *Pinus nigra* spp. *laricio* (Corsica/France). *Chemical Geology* **308–309**: 40–48.

Tesfaye G, Teketay D, Fetene M, Beck E. 2010. Regeneration of seven indigenous tree species in a dry Afromontane forest, southern Ethiopia. *Flora* **205**: 135–143.

Tesfaye G, Teketay D, Fetene M, Beck E. 2011. Phenology of seven indigenous tree species in a dry Afromontane forest, southern Ethiopia. *Tropical Ecology* **52**: 229–241.

Verheyden A, Kairo JG, Beeckman H, Koedam N. 2004. Growth rings, growth ring formation and age determination in the mangrove *Rhizophora mucronata*. *Annals of Botany* **94**: 59–66.

Volland-Voigt F, Bräuning A, Ganzhi O, Peters T, Maza H. 2011. Radial stem variations of *Tabebuia chrysantha* (Bignoniaceae) in different tropical forest ecosystems of southern Ecuador. *Trees* **25**: 39–48.

Warren CR, McGrath JF, Adams MA. 2001. Water availability and carbon isotope discrimination in conifers. *Oecologia* **127**: 476–486.

Williams AP, Funk C, Michaelsen J, Rauscher SA, Robertson I, Wils THG, Koprowski M, Eshetu Z, Loader NJ. 2011. Recent summer precipitation trends in the Greater Horn of Africa and the emerging role of Indian Ocean sea surface temperature. *Climate Dynamics* **39**: 2307–2328.

Wils THG, Robertson I, Eshetu Z, Koprowski M, Sass-Klaassen UGW, Touchan R, Loader NJ. 2010. Towards a reconstruction of Blue Nile baseflow from Ethiopian tree rings. *The Holocene* **20**: 837–848.

Wils THG, Sass-Klaassen UGW, Eshetu Z, Bräuning A, Gebrekirstos A, Couralet C, Robertson I, Touchan R, Koprowski M, Conway D, *et al.* 2011. Dendrochronology in the dry tropics: the Ethiopian case. *Trees* **25**: 345–354.